

Electronic Supplementary Information

Direct Mapping of Chemical Oxidation of Individual Graphene Sheets through Dynamic Force Measurements at Nanoscale

Jens P. Froning, Petr Lazar, Martin Pykal, Qiang Li, Mingdong Dong*, Radek Zbořil*, Michal Otyepka1*

Increase of defects owing to UV/Ozone treatment

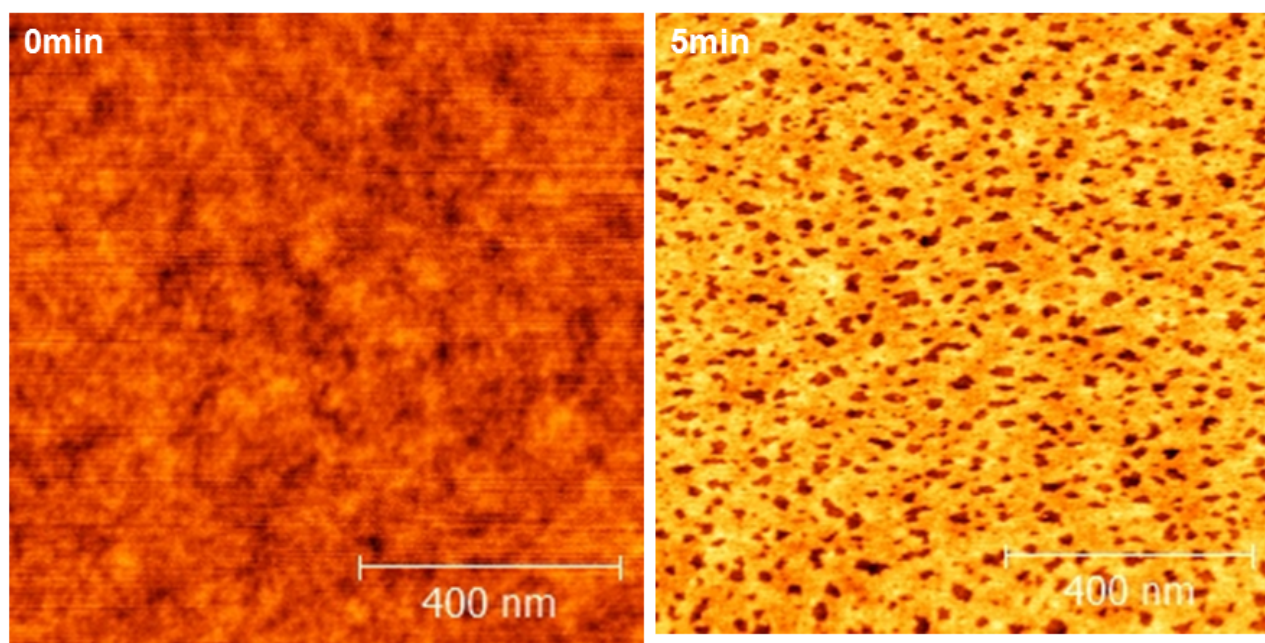


Figure S-1 AFM topography images of single layer graphene on Silicon dioxide before and after 5 min in the UV/Ozone cleaner.

Prior to the main experiment, the effect the UV/ozone cleaner from Bioforce was tested on graphene, where the topography showed defects after just 5 min of treatment as revealed by the AFM (Fig. S-1). Therefore, 1 min was selected for the intervals of the treatment cycles, which is enough time to start the reaction without causing too much damage to the graphene.

*Corresponding Authors: dong@inano.au.dk; radek.zboril@upol.cz; michal.otyepka@upol.cz

Jump into contact range

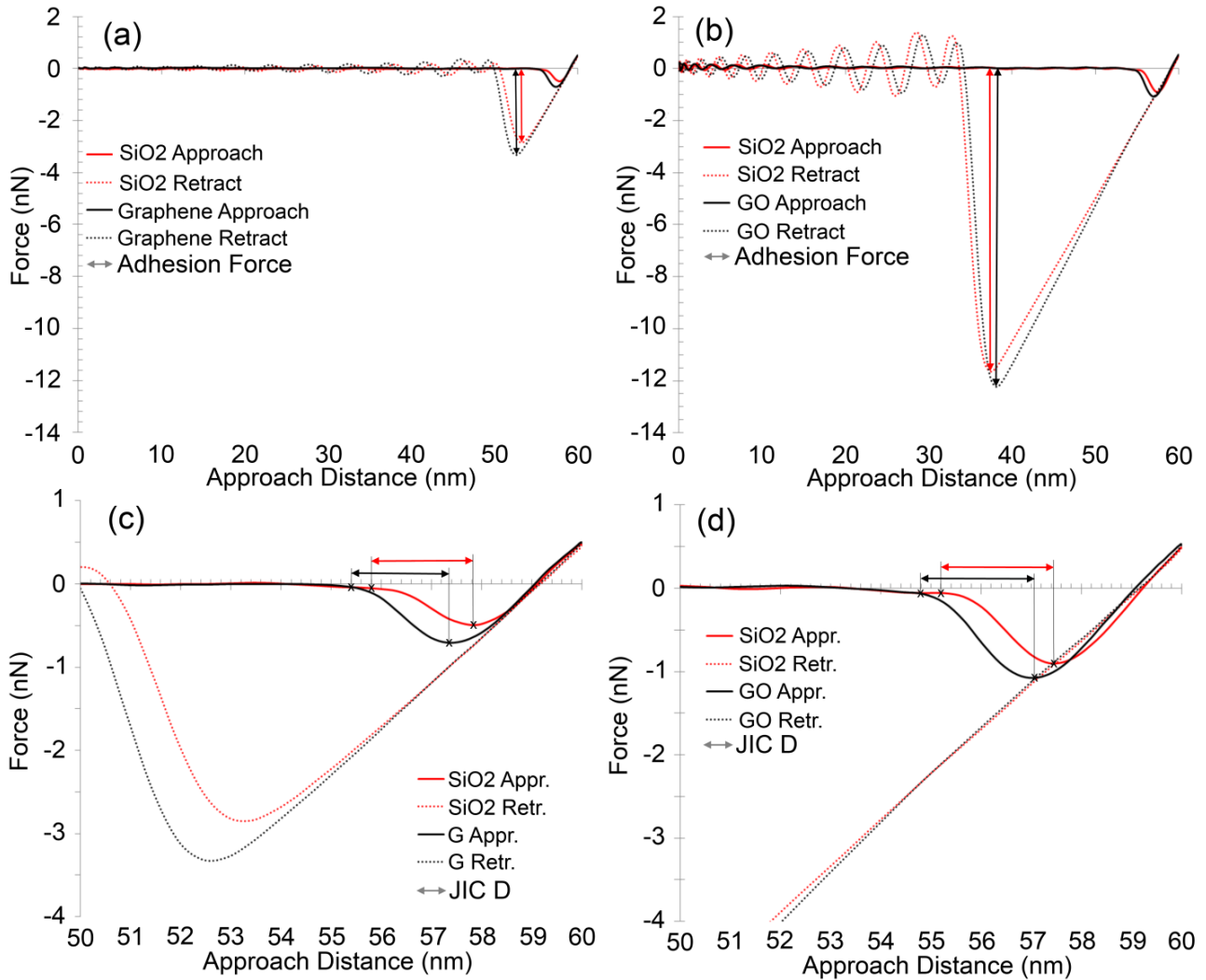


Figure S-2 Force curve on (a and c) untreated graphene (G) and (b and d) 1 min oxidized graphene (GO) on Silicon dioxide (SiO₂). The total adhesion force is marked by a double arrow in (a) and (b), and so is the jump-into-contact distance (DJIC) in (c) and (d). (c) and (d) are enlargements the spectra (a) and (d) to make the estimation of DJIC easier.

The stabilization of the environmental conditions ensures that the measurements are not influenced by changing laboratory conditions. Since we are oxidizing graphene a formation of the water layer at the surface might not be so unlikely. Both for graphene and graphene oxide we experienced alterations of the adhesion force depending on the environmental conditions. The jump into contact distance (D_{JIC}) functions as an indicator, since the interaction distance can be estimated from it for the different surfaces (Fig. S-2). If there is a water layer and if it changes due to the oxidation, D_{JIC} would differ. The jump-into-contact distance for all measurements was between 2 nm to 2.2 nm (Fig. S-2c&d), which means that the long range interaction force remain comparable and that the major contribution to the adhesion is caused by short range interaction with the sample surface in the range of 0.3-0.6 nm.

AFM characterization of graphene flake

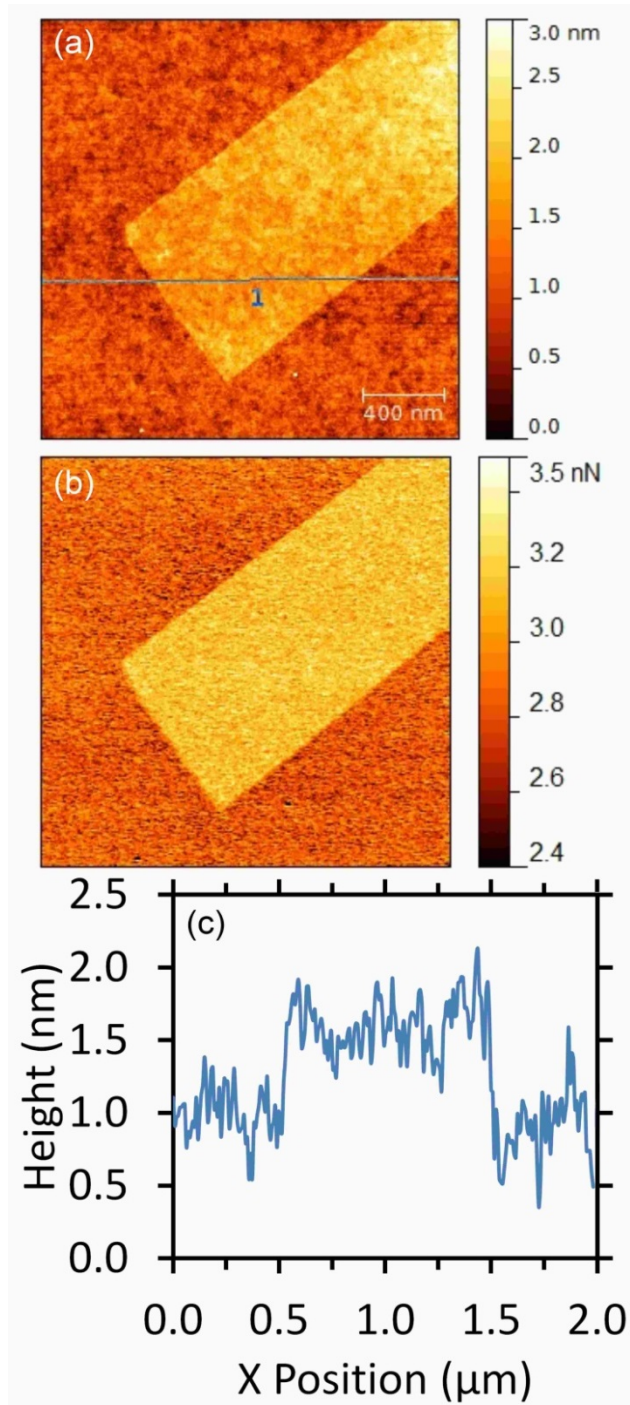


Figure S-3 Confirmation of single layer graphene by AFM. (a) The AFM topography of a single flake was taken simultaneously with (b) the adhesion map. (c) The height profile was measured along the line noted 1 in (a) and the height of the graphene was estimated to be about $(0.62 \pm 0.07) \text{ nm}$ on the silicon dioxide..

The presence of single layered graphene was confirmed by the line profile taken across each flake as it can be

seen in the Figure S-3. We wanted to ensure that all the flakes are comparable in the height before treating them together in the UV/ozone cleaner. The flake from Figure S-3 showed a similar behavior as the flake illustrated in the main text (Fig. S-4).

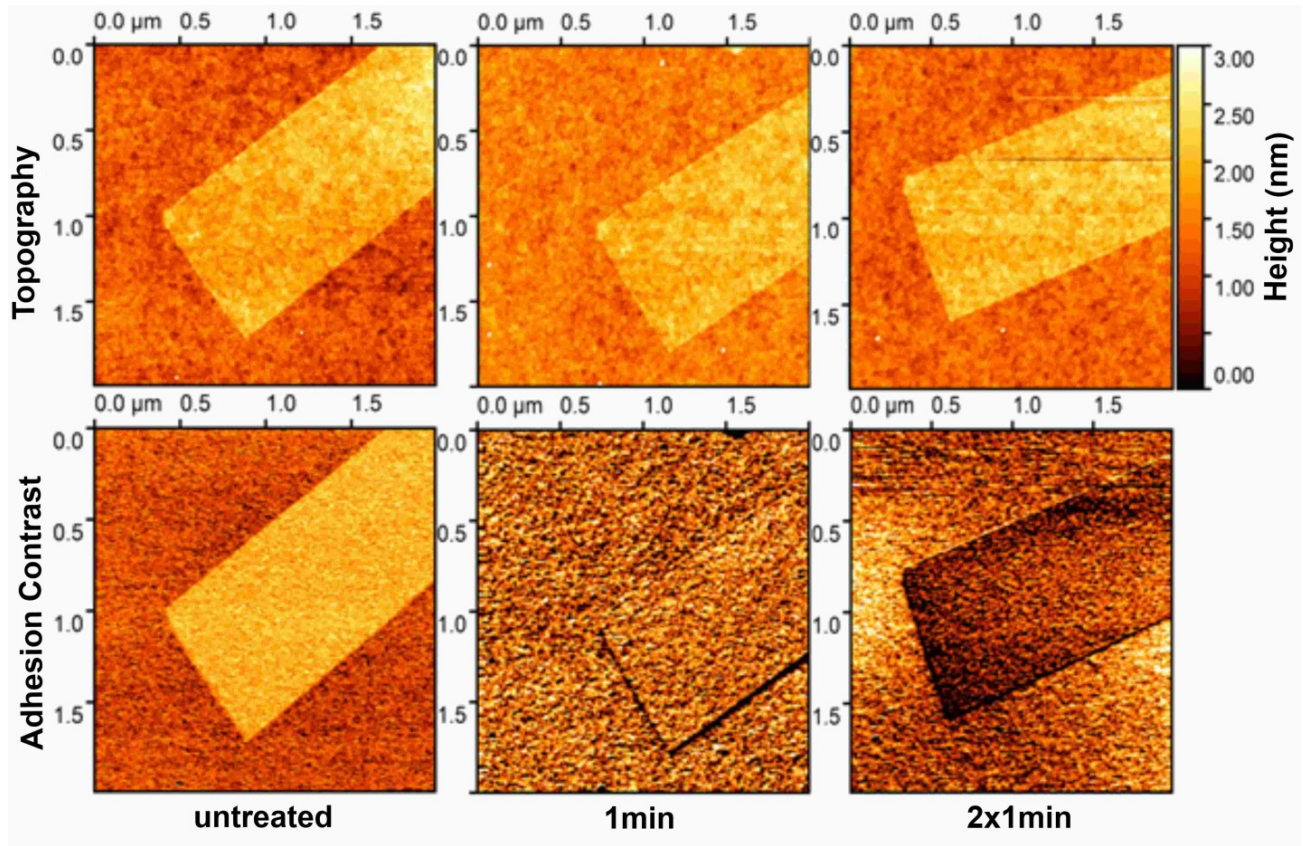


Figure S-4 Single layer graphene flake named sample II, which was treated twice along with Sample I by UV/ozone.

Alterations in the adhesion force caused by contamination

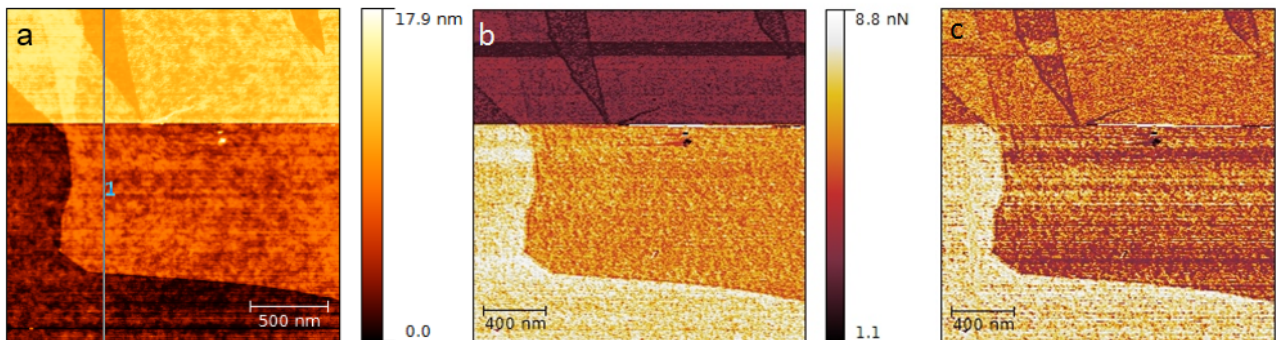


Figure S-5 PeakForce QNM scan of a single layer graphene flake on SiO₂ showing a sudden alteration of the adhesion force. The alteration is visible in (a) topography, (b) adhesion map, and (c) adhesion contrast. The scan was done line by line from the bottom to the top.

As in all SPM techniques, the probe is interacting with the sample surface during an AFM scan. With respect to the adhesion different probes have a different strength and different selectivity. In the main text, we showed had two different probes react different to the oxidation of the sample surface. The difference between a sharp silicon tip and a spherical silica probe is shown in the total adhesion not only in magnitude but also in response to the first oxidation step. The first can be explained through the bigger area of contact for the spherical probe and various theoretical models ¹⁻³. We would like to discuss this by looking at a change of the probe during a measurement.

Such changes can include the probe's shape and possible modification of its surface chemistry. Adhesion and its selectivity change when the surface chemistry of the probe is altered ^{4,5}. A different selectivity is observable as altered adhesion contrast. Figure S-5 shows a natural incident where the probe surface changed suddenly. In amplitude modulated tapping mode, a sudden change in phase imaging could be caused by the oscillation probe jumping from the repulsive region to the attractive region. The amplitude would be the same but the phase would be different. The AFM mode used by us however works without an oscillating probe and only in the repulsive range, therefore such a jump was most likely caused by contamination. The sudden change is visible in three ways.

In the topography, the height seems to increase from one line to the other (Fig. S-5a), and the adhesion drops simultaneously (Fig. S-5b). Since the actual surface topography does not change so dramatically, a plausible explanation is that the probe got rid of some contamination causing the feedback loop to register a sudden change in the probe surface distance. Because of the compensation for the sudden difference in distance, the topography shows a sudden increase in height. The decreasing adhesion for the same surfaces on the sample also indicates a sudden change of the probe. Beside the drop in the adhesion, also the selectivity of the adhesion changes as it can be seen in the adhesion contrast (Fig. S-5c). Unfortunately, it is impossible to avoid picking up contamination from certain samples, but the adhesion is a good indicator.

Scanning with spherical probe

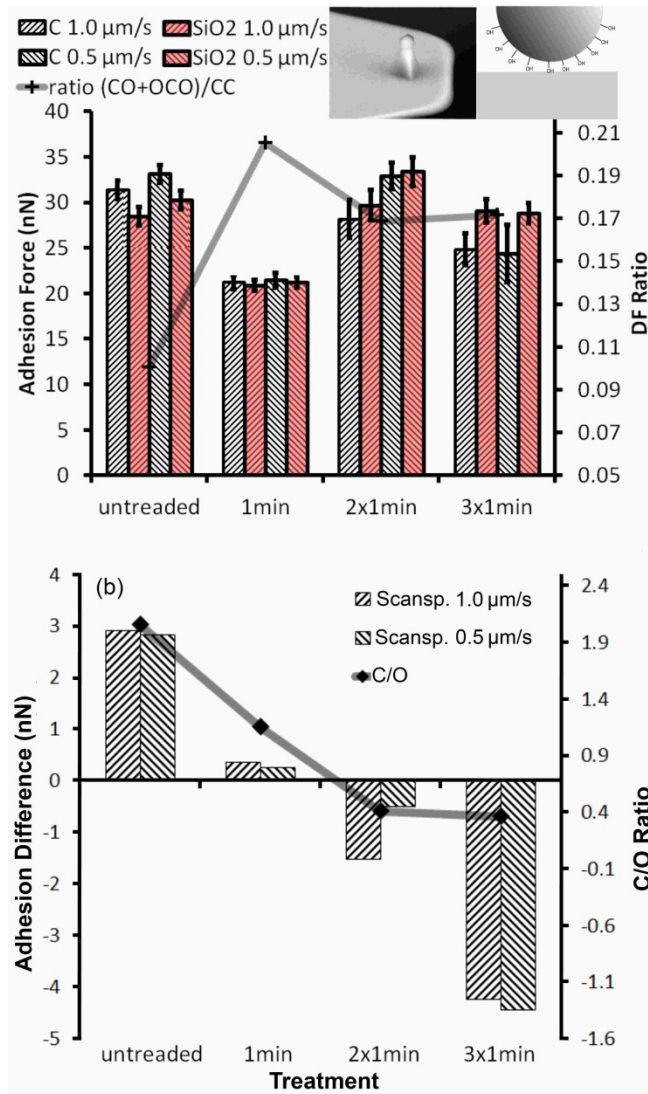


Figure S-6 Adhesion measurements acquired with a spherical probe (see inset for SEM image and schematic) on the samples after UV/ozone treatment compared with their XPS measurements. (a) Total adhesion force with respect to treatment of graphene (black columns) and SiO₂ (red columns) measured at different scan speeds with a spherical probe. The adhesion is directly compared to the inverse degree of functionalization calculated from the XPS (gray line). (b) Adhesion difference between substrate and flake shown together with the C/O ratio obtained from XPS for all samples.

In the main text, the behavior of a sharp silicon probe was shown with respect to the oxidation of the graphene flake. A similar behavior was the case with another probe, a colloid silica probe with a different surface chemistry. To verify that the interpretation in the main text was robust and experiments were repeatable, several graphene flakes comparable to the one shown in Figure 3 were scanned with this larger silica colloid probe (Fig. S-6). We expected a different behavior related to the different probe material and surface chemistry as it had been reported for using different functionalized probes ⁶ (further details in the

ESM), This was confirmed by the adhesion force. The measured adhesion force was much stronger owing to the increased contact area of the colloid probe, in agreement with various theoretical models (Johnson-Kendall-Roberts (JKR) ¹, Derjaguin-Muller-Toporov (DMT) ², Tabor ³). Use of the sharp probe enhanced the resolution, but the images were more influenced by scanning speed and surface roughness than when using the colloid probe, especially for the roughest flake (Figs. 4(a) and S-6(a)). However, when a high scan speed was used, structural features were averaged out and the contrast results became more comparable to the ones obtained with the larger colloid probe.

The behavior of the adhesion contrast with the respect to the C/O ratio is similar to the sharp probe illustrated in the main text (Fig. S-6). For both probe, the increase in oxidation means a decrease in the contrast between the SiO₂ substrate and the graphene flake. Unlike the sharp probe the spherical probe is not influence as much as the sharp probe by the defects occurring in the last oxidation cycle. This is caused by the natural average of the larger contact area, which is provided by the spherical probe.

Detailed sample preparation

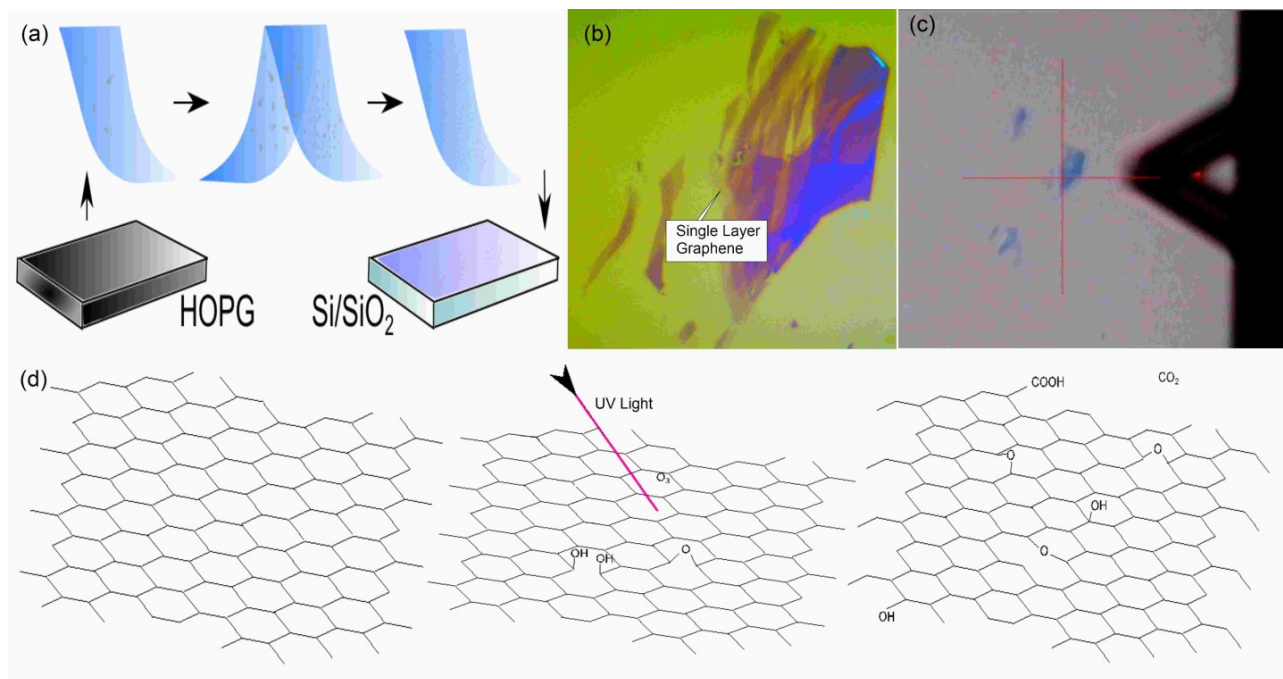


Figure S-6 Preparation and treatment of the graphene samples on SiO₂ film. (a) A scheme of the scotch tape method where the tape is used to remove and exfoliate the graphite for the deposition on the substrate. The graphite stuck on the tape is exfoliated by folding the tape back on itself and splitting it again. (b) Due to the SiO₂ film, the optical microscope can reveal few layer and single layer graphene. (c) The regions of interest can be used to position the AFM probe. (d) After confirming the graphene layer by height, the treatment with ultra violet light and ozone as oxidation agent is conducted, where the high energy photons activate the carbon atoms for the reaction with the agent.

The graphene was prepared by mechanical exfoliation of HOPG using the scotch tape method. From the tape it was deposited on a 285nm thick silicon dioxide substrate to allow localization of the single layer graphene by optical microscopy (Fig. S-6a-c). From the line profile, the height of the graphene was estimated to be around (0.62 ± 0.07) nm on the silicon dioxide film (Fig. S-4).

During the experiment, the same probe was used to monitor the alternating interaction forces for the same flakes as result of the treatment. The ultra violet light activates the carbon for the reaction with ozone creating the functional groups at the graphene depending on the treatment time (Fig. S-6d). After each treatment cycle, the same flake was aligned with the AFM probe by the optical microscope.

A flow chart of the treatment experiment is given to clarify in which way the experiment was conducted (Fig. S-7). All samples were treated together in the UV/ozone cleaner in order to ensure that the samples were treated equally. The sample presented in the main text is Sample I in the chart. The results of Sample II can be seen in Figure S-4, which was only treated two times. Still the flake shows similar behavior as the one presented in the main text.

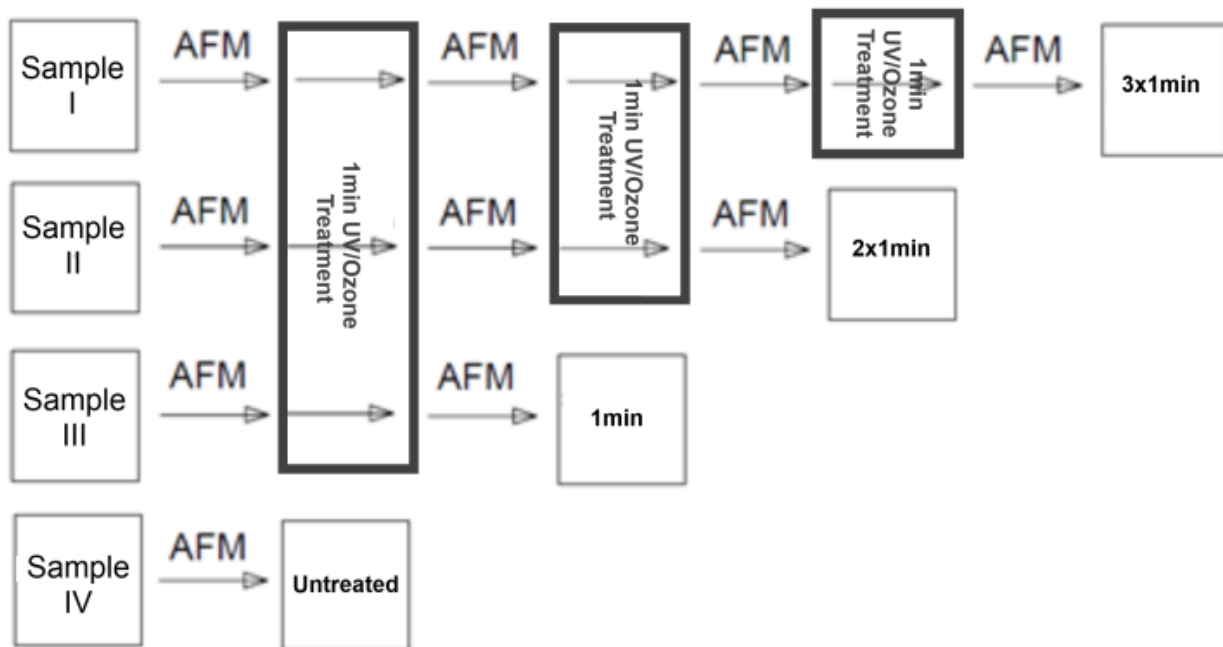


Figure S-7 Flow chart of the main experiment. Four comparable samples were treated together in the UV/Ozone cleaner. After each cycle one of the samples was removed and kept at the current state as a reference and for later characterization experiments. After each cycle all the remaining samples were scanned with the same AFM probe regarding topography and adhesion forces.

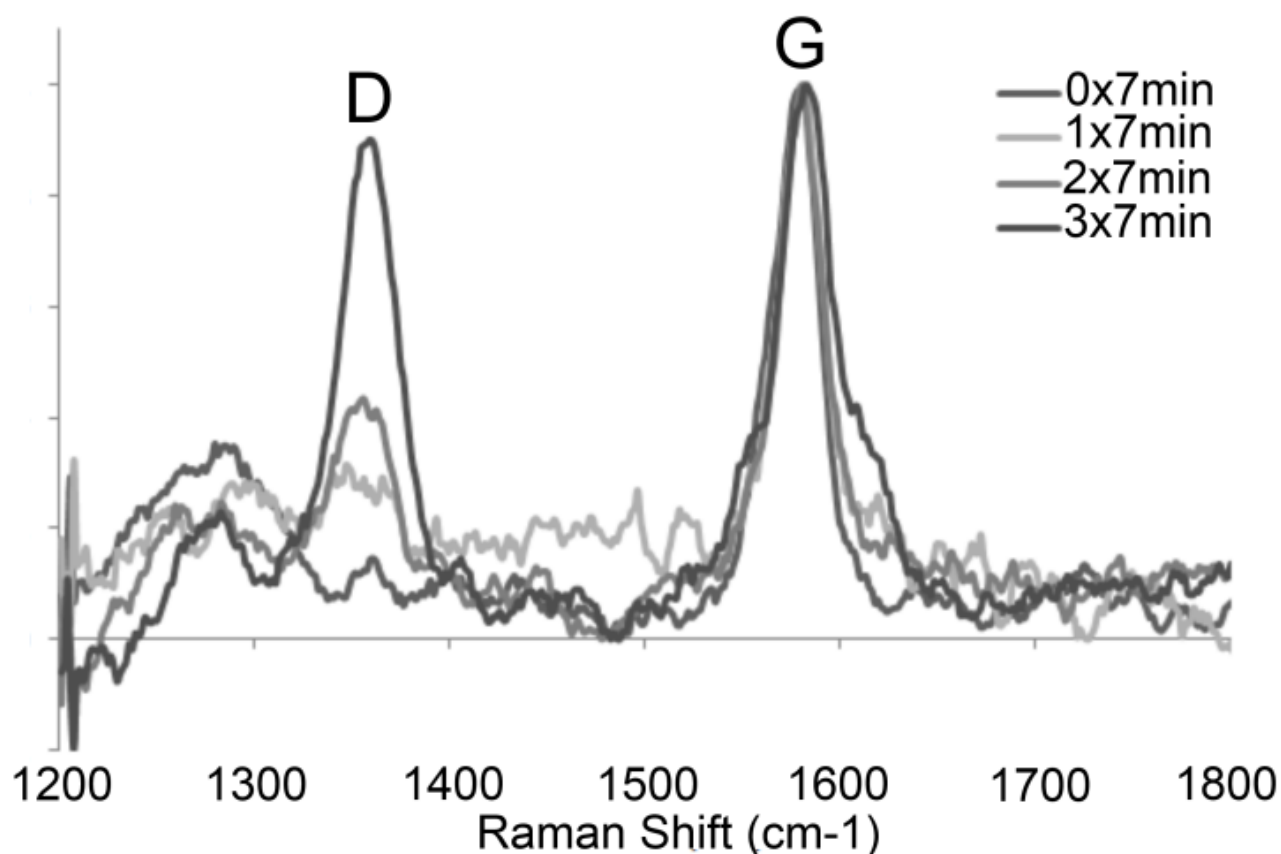


Figure S-8 Raman Spectra of the G and D band of CVD graphene treated with UV/Ozone. The sample were treated with a different cleaner where each cycle time was 7 min instead of 1 min due to the weaker oxidation

Figure S-7 is an example, how the degree of functionalization can be monitored by Raman spectroscopy. The samples were also treated by UV/ozone in a similar machine as the one from Bioforce, the UVO-Cleaner 42 from Jelight Comp. US. This cleaner seems to be less effective, that is why the time for the treatment cycle was increased to 7 min instead of 1 min. The Raman spectrum shows an increase in the sp^3 hybridization since the D band becomes stronger compared to the G band.

Dynamic Force mapping

A MultiMode8 atomic force microscope from Bruker, Santa Barbara, with PeakForce Quantitative Nanomechanical mapping (PF), was used to collect the adhesion properties and topography data. Its fast recording of force spectra makes the interpretation in respect to the interaction easier than phase imaging⁷. Since phase imaging is looking at the change in the oscillation phase of the cantilever, one needs to consider parameters of the oscillation during the measurement, for example the free amplitude, set point settings, and so forth. Force spectroscopy works with a static probe and any kind of cantilever oscillation should be minimized.

The idea of force spectroscopy is to monitor the interaction between probe and sample through the bending

of the cantilever while the distance between probe and sample is being altered. For fast force spectroscopy, such as PF, the spectra are collected with a sampling frequency up to 8 kHz, where the probe-sample distance follows a sinusoidal modulation. Since the cantilever's resonance frequency is much higher, resonance oscillation hardly interferes with the measurement, but is still visible as a ringing noise (Fig. S-9), when the probe is released from the sample. Due to the damping the ringing fades out before the next spectrum is collected.

Another advantage of the fast force spectroscopy is that the repulsive interaction between probe and surface is not only monitored but controlled. The maximal repulsion force is the set point criteria for the feedback loop controlling the probe-sample distance. By keeping the maximal repulsion constant, the feedback loop follows the surface topography while force spectra for each point are recorded. For our experiment, the sampling frequency for the force spectra was 2 kHz, while each height profile line was recorded with 1 Hz scan rate.

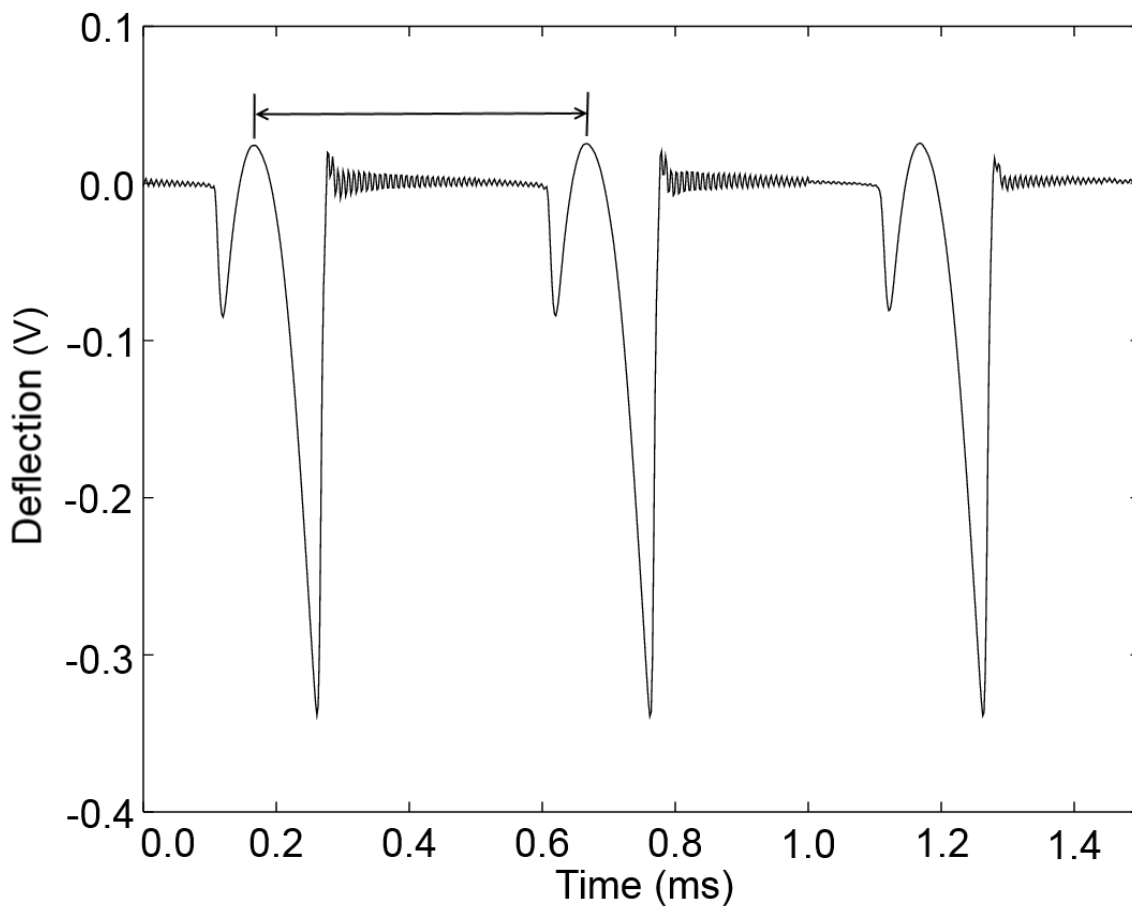


Figure S-9 An example of the recorded deflection signal during the PeakForce measurement. The double arrow marks the period length of the sinus modulation with 2 kHz frequency, while the so called “ringing” after probe release is related to the resonance frequency and the damping of the cantilever. Due to the bending direction of the cantilever, repulsive forces show up as positive values, while the resting position is set to be zero.

Stabilization by Nitrogen flow

Since we are dealing with a humidity sensitive interaction ⁸, it is necessary to stabilize the environmental conditions. Otherwise we would not be sure that the adhesion fluctuations were caused by the chemical modification of the surface. For this purpose, the crucial parts of the system were sealed from the lab environment with a hood and kept under a constant nitrogen flow. The flow was big enough to stabilize the conditions, yet not strong enough to cause extra noise. Before each measurement, the system was given at least 20 min to reach equilibrium, a time frame estimated during testing of the method. Between the measurements the temperature and the humidity were measured with a simple sensor, which was placed inside the hood next to the sample (Fig. S-10).

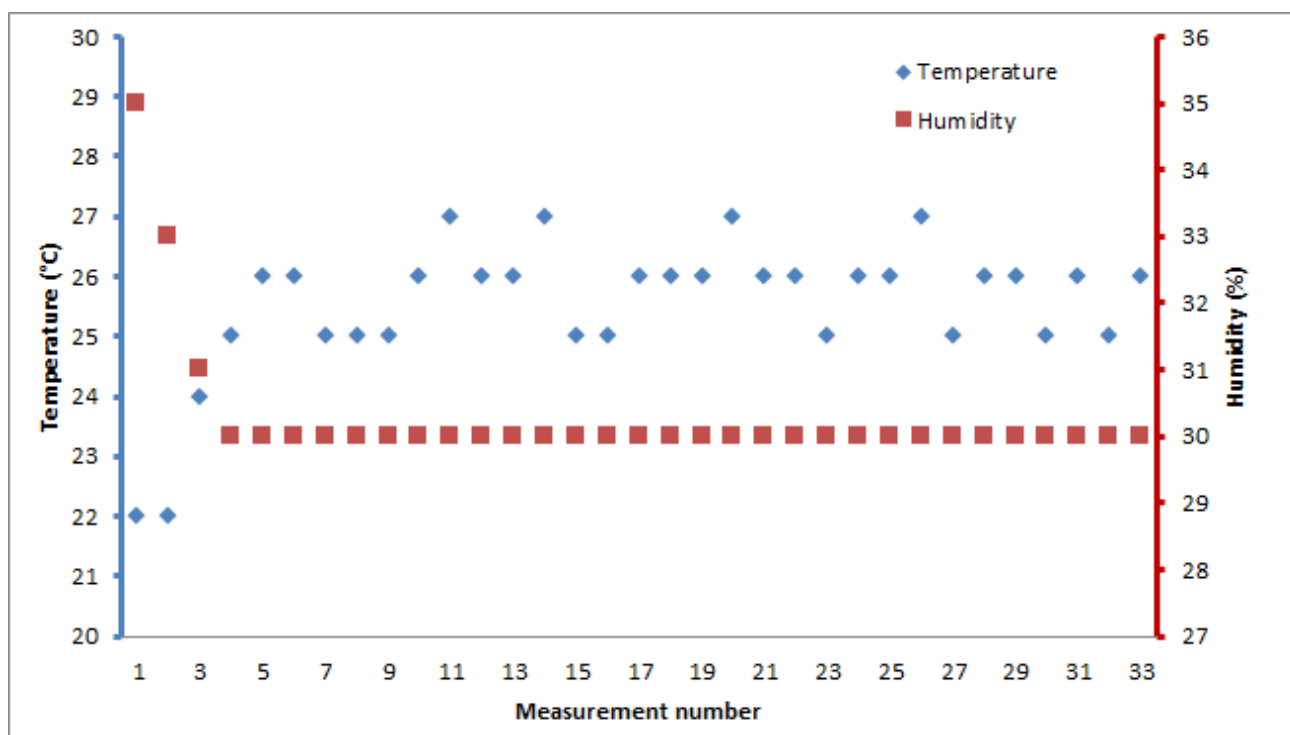


Figure S-10 The temperature and humidity data collected before and between the adhesion measurements to ensure a stabilized system.

References

1. K. L. Johnson, K. Kendall and A. D. Roberts, *Proceedings of the Royal Society of London A: Mathematical, Physical and Engineering Sciences*, 1971, 324, 301-313.
2. B. V. Derjaguin, V. M. Muller and Y. P. Toporov, *J. Colloid. Interf. Sci.*, 1975, 53, 314-326.
3. D. Tabor, *J. Colloid. Interf. Sci.*, 1977, 58, 2-13.
4. P. Lazar, S. Zhang, K. Safarova, Q. Li, J. P. Froning, J. Granatier, P. Hobza, R. Zboril, F. Besenbacher, M. D. Dong and M. Otyepka, *ACS Nano*, 2013, 7, 1646-1651.

5. M. Hibino and T. Nakano-Nishida, *J. Nanosci. Nanotechnol.*, 2014, 14, 3080-3086.
6. Y. Okabe, U. Akiba and M. Fujihira, *Appl. Surf. Sci.*, 2000, 157, 398-404.
7. W. Deng, G. M. Zhang, M. F. Murphy, F. Lilley, D. M. Harvey and D. R. Burton, *Microsc. Res. Tech.*, 2015, 78, 935-946.
8. H. S. Morris, V. H. Grassian and A. V. Tivanski, *Chem. Sci.*, 2015, 6, 3242-3247.